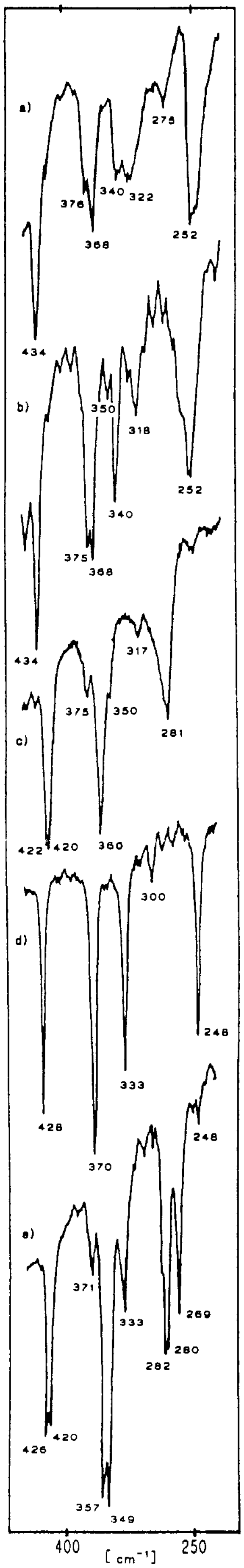

Figure 2. Far-infrared spectral bands of *cis*- and *trans*-Rh(bpy)$_2$XY^{n+} complexes: (a) [*trans*-Rh(bpy)$_2$Cl]$_2$(H$_5$O$_3$)(ClO$_4$)$_3$; (b) [*trans*-Rh(bpy)$_2$(H$_2$O)Cl](ClO$_4$)$_2$; (c) [*cis*-Rh(bpy)$_2$(H$_2$O)Cl](ClO$_4$)$_2$·H$_2$O; (d) [*trans*-Rh(bpy)$_2$Cl$_2$]Cl; (e) [*cis*-Rh(bpy)$_2$Cl$_2$]Cl·2H$_2$O.

plexes as in the literature[14] and are in good agreement with those for related complexes containing the RhN$_4$XY^{n+} configuration. Reduction of symmetry (from D_{2h} for trans to C_2 for cis, X = Y) leads to a loss of vibrational degeneracy and a splitting of the only infrared-active antisymmetric Rh–Cl stretching mode A$_{2u}$ into the symmetric A$_1$ and the antisymmetric B$_1$ mode. Translabilization effects of coordinated chloride should shift the Rh–Cl vibration for the *trans*-dichloro complex to lower energy compared to that for the *cis*-dichloro species. However, the higher frequency of the 370-cm^{-1} band observed for the trans species compared to the 357- and 349-cm^{-1} bands for the cis species may indicate a strengthening of the Rh–Cl bond attributed to a π-overlap between the filled 3p orbitals of Cl and an extended π-system of the two nearly coplanar bpy ligands. Group frequency arguments suggest a single infrared-active Rh–N stretching vibration for the trans complex, and we assign the sharp band at 248 cm^{-1} of the *trans*-dichloro complex to the Rh–N vibration. It should degenerate into four vibrations for the cis complex, of which one is observed clearly at 269 cm^{-1} and three fall in the 290–280-cm^{-1} region.

In the case of a mixed trans complex with X $\neq$ Y the symmetry is also C_2. The two X–Rh–Y stretching modes are both of A$_1$ symmetry and can be divided into one in which the Rh–X stretch contributes mainly and one in which the Rh–Y stretch is more important. We assign the band at 368 cm^{-1} of the *trans*-chloro–aqua complex to the Rh–Cl vibration. From a comparison of the cis and trans structures, this band also shows a shift to higher energy as for the *trans*-dichloro complex.

By way of comparison we find a strengthening of the Rh–Cl bond when going from the cis to the trans complexes, but the opposite trend for the Rh–N bond. The broad band at 281 cm^{-1} for the *cis*-chloro–aqua complex can be located at 252 cm^{-1} for the trans complex.

Present uncertainties in the interpretation of the spectra in Figure 2 concern the bands in the 340–320-cm^{-1} region. It is also not possible to determine the symmetry species of the bonds observed in the infrared spectra since Raman data are still lacking.

Acknowledgment. We gratefully acknowledge financial support from the Deutsche Forschungsgemeinschaft and the Fonds der Chemischen Industrie. We also wish to acknowledge the University of Bochum for providing facilities to record the far-infrared spectra.

Supplementary Material Available: A table of anisotropic thermal parameters and complete infrared spectra of the species indicated in Figure 2 (6 pages); a table of observed and calculated structure factors (32 pages). Ordering information is given on any current masthead page.

---

(14) Gillard, R. D.; Heaton, B. T. *J. Chem. Soc. A* **1969**, 451.

Contribution from the Department of Chemistry,
Purdue University, West Lafayette, Indiana 47907-3699

Crystal and Molecular Structure of [Cu(bcp)$_2$]BF$_4$·CH$_3$OH (bcp = 2,9-Dimethyl-4,7-diphenyl-1,10-phenanthroline)

Frank K. Klemens, Phillip E. Fanwick, Jodi K. Bibler,
and David R. McMillin*

Received January 27, 1989

Complexes of the type Cu(phen)$_2^+$ and its variants, where phen denotes 1,10-phenanthroline, comprise a class of compounds in which there has been wide ranging interest, as is evident from reports on electronic spectra,[1–4] redox properties,[5–9] photochemistry

---

(1) Williams, R. J. P. *J. Chem. Soc.* **1955**, 137–145.
(2) Day, P.; Sanders, N. *J. Chem. Soc. A* **1967**, 1536–1541.

0020-1669/89/1328-3076$01.50/0 © 1989 American Chemical Society

Table I. Crystal Data and Data Collection Parameters

fw	903.31	ρ_{calcd}, g/cm^3	1.361
formula	$CuF_4ON_4C_{53}BH_{44}$	$F(000)$	1872.0
space group	$P2_1/c$ (No. 14)	crystal dimens, mm	0.85 × 0.28 × 0.06
a, Å	11.131 (3)	μ, cm^{-1} (Mo K$_\alpha$)	5.54
b, Å	21.454 (4)	λ, Å	0.71073
c, Å	18.900 (3)	temp, °C	−89
β, deg	102.34 (2)	transm coeff	1.00–0.455
V, Å^3	4409 (3)	$R(F_o)$	0.056
Z	4	$R_w(F_o)$	0.073

and photophysics,[10-14] molecular structure,[15,16] and—under appropriate conditions—artificial nuclease activity.[17-19] The chemical and physical properties of the ion are dramatically influenced by substituents on the phen ligand, and we have been interested in the unique effects associated with aryl substituents at the 4- and 7-positions of the phenanthroline ring. Thus, when phenyl groups are present, the absorptivities of the CT transitions increase markedly due to the extension of the dipole moment connected with CT excitation.[4] Recent work also suggests that the phenyl substituents significantly influence the way in which the copper(I) complex binds to DNA.[18,20] Evidently, the presence of the 4,7-phenyls promotes intercalation into the double helix of B form DNA, even though steric interactions involving the exocyclic hydrogens should prevent the phenyl groups from lying in the plane of the phenanthroline ring system. To obtain more insight into the steric requirements posed by the phenyl groups, we have solved the structure of $[Cu(bcp)_2]BF_4\cdot CH_3OH$, where bcp denotes 2,9-dimethyl-4,7-diphenyl-1,10-phenanthroline.

Experimental Section

Synthesis. The ligand was purchased from Aldrich and was not further purified. The copper compound was obtained as a solid when an aqueous methanol solution containing 1 mmol of $Cu(BF_4)_2\cdot H_2O$ was reduced with excess sodium L-ascorbate (Aldrich) and then combined with 2 mmol of bcp dissolved in acetone. Brick red, needlelike crystals of $[Cu(bcp)_2]BF_4\cdot CH_3OH$ were formed by evaporation of an acetone/methanol (3:1 by volume) solution.

Diffraction Methods. The crystals were mounted on a glass fiber with epoxy resin. During data collection the ratio of peak-counting time to background-counting time was 2:1, and for intense reflections an attenuator was placed in front of the detector. Diffraction measurements were made, and data collection was achieved with an Enraf-Nonius CAD4 diffractometer; all calculations were performed on a PDP-11 computer with Enraf-Nonius SDP software. Mo Kα radiation (λ = 0.71073 Å) was used in conjunction with a graphite monochromator. The cell constants (Table I) and the orientation matrix were obtained from analysis of 25 reflections in the range 17.55° < θ < 20.83°. The structure was determined from a least-squares minimization of the function $\sum w(\Delta F)^2$, where $\Delta F = |F_o| - |F_c|$ and w is the weighting factor. The weighting factor was calculated by using $w = 4(F^2)/(\sigma_{F^2})^2$ in which $\sigma_{F^2} = [\sigma_I^2 + (PF^2)^2]^{0.5}$, where σ_I comes from counting statistics and P = 0.04. Neutral-atom scattering factors were used for all atoms.[21]

Table II. Positional Coordinates for $[Cu(bcp)_2]BF_4\cdot CH_3OH$

atom	x	y	z	B, Å^2
Cu	0.13971 (7)	0.19989 (4)	0.35385 (3)	2.81 (1)
N(100)	0.1782 (4)	0.1425 (2)	0.2771 (2)	2.5 (1)
N(190)	0.0098 (4)	0.2307 (2)	0.2693 (2)	2.5 (1)
N(200)	0.0924 (4)	0.1607 (2)	0.4419 (2)	2.1 (1)
N(290)	0.2542 (4)	0.2492 (2)	0.4309 (2)	2.4 (1)
C(101)	0.0980 (5)	0.1493 (3)	0.2117 (3)	2.5 (1)
C(102)	0.1007 (5)	0.1124 (3)	0.1507 (3)	2.6 (1)
C(110)	0.2641 (5)	0.0986 (3)	0.2820 (3)	2.7 (1)
C(111)	0.3457 (6)	0.0875 (3)	0.3556 (3)	4.0 (2)
C(120)	0.2791 (5)	0.0627 (3)	0.2225 (3)	2.7 (1)
C(130)	0.1977 (5)	0.0686 (3)	0.1564 (3)	2.9 (1)
C(140)	0.0045 (6)	0.1198 (3)	0.0880 (3)	3.3 (1)
C(150)	−0.0792 (6)	0.1655 (3)	0.0837 (3)	3.5 (1)
C(160)	−0.1577 (5)	0.2607 (3)	0.1386 (3)	3.0 (1)
C(170)	−0.1562 (6)	0.2919 (3)	0.2025 (3)	3.3 (1)
C(180)	−0.0741 (6)	0.2765 (3)	0.2669 (3)	2.9 (1)
C(181)	−0.0734 (6)	0.3113 (3)	0.3356 (3)	4.0 (2)
C(191)	0.0073 (5)	0.1972 (3)	0.2076 (3)	2.7 (1)
C(192)	−0.0769 (6)	0.2090 (3)	0.1420 (3)	3.0 (1)
C(201)	0.1535 (5)	0.1870 (2)	0.5048 (3)	2.0 (1)
C(202)	0.1378 (5)	0.1681 (3)	0.5739 (3)	2.0 (1)
C(210)	0.0141 (5)	0.1147 (3)	0.4457 (3)	2.5 (1)
C(211)	−0.0533 (6)	0.0877 (3)	0.3748 (3)	3.2 (1)
C(220)	−0.0005 (5)	0.0905 (3)	0.5119 (3)	2.5 (1)
C(230)	0.0606 (5)	0.1154 (3)	0.5764 (3)	2.1 (1)
C(240)	0.1974 (5)	0.2033 (3)	0.6355 (3)	2.3 (1)
C(250)	0.2763 (5)	0.2499 (3)	0.6300 (3)	2.4 (1)
C(260)	0.3972 (5)	0.3092 (3)	0.5531 (3)	2.4 (1)
C(270)	0.4096 (6)	0.3216 (3)	0.4835 (3)	2.9 (1)
C(280)	0.3369 (5)	0.2919 (3)	0.4229 (3)	2.9 (1)
C(281)	0.3515 (7)	0.3064 (4)	0.3480 (3)	4.4 (2)
C(291)	0.2404 (5)	0.2354 (3)	0.4989 (3)	2.0 (1)
C(292)	0.3064 (5)	0.2649 (3)	0.5617 (3)	2.1 (1)

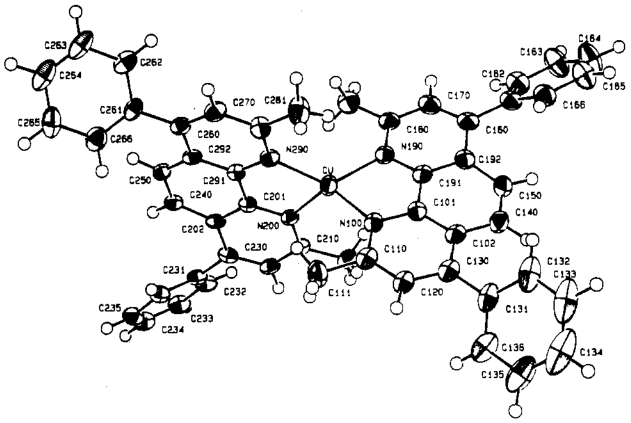

Figure 1. ORTEP diagram along with the numbering scheme for $[Cu(bcp)_2]BF_4\cdot CH_3OH$.

Crystal Data. An elongated box-shaped crystal of $[Cu(bcp)_2]BF_4\cdot CH_3OH$ with approximate dimensions of 0.85 × 0.28 × 0.06 mm was used. The unit cell was found to be monoclinic, and the space group was confirmed to be $P2_1/c$ (No. 14) by the refinement. Pertinent crystal data are listed in Table I. The data were collected at a temperature of −89 °C, which was controlled with a flow of cold nitrogen gas by using an Enraf-Nonus Model 524 temperature regulator. The ω–2θ scan technique was used with a 2θ range of 4.00–45.00°. The scan rate was determined by the instrument, and the scan width was 0.59° + (0.35 tan θ)° with a takeoff angle of 1.90°. The scan range was corrected for the separation of the Kα doublet.[22]

A total of 5930 unique reflections were collected with h, k, and l limits of 0–11, 0–23, and −20–19, respectively. In all, 3648 reflections met the

---

(3) Ichinaga, A. K.; Kirchhoff, J. R.; McMillin, D. R.; Dietrich-Buchecker, C. O.; Marnot, P. A.; Sauvage, J. P. *Inorg. Chem.* **1987**, *26*, 4290–4292.

(4) Phifer, C. C.; McMillin, D. R. *Inorg. Chem.* **1986**, *25*, 1329–1333.

(5) Hawkins, C. J.; Perrin, D. D. *J. Chem. Soc.* **1962**, 1351–1357.

(6) Hawkins, C. J.; Perrin, D. D. *J. Chem. Soc.* **1963**, 2996–3002.

(7) Al-Shatti, N.; Lappin, A. G.; Sykes, A. G. *Inorg. Chem.* **1981**, *20*, 1466–1469.

(8) Yandell, J. K. In *Copper Coordination Chemistry: Biochemical and Inorganic Perspectives*; Karlin, K. D., Zubieta, J., Eds.; Adenine Press: Guilderland, NY, 1982; pp 157–166.

(9) Davies, K. M.; Byers, B. *Inorg. Chem.* **1987**, *26*, 3823–3825.

(10) Ahn, B. T.; McMillin, D. R. *Inorg. Chem.* **1981**, *20*, 1427–1432.

(11) Gamache, R. E., Jr.; Rader, R. A.; McMillin, D. R. *J. Am. Chem. Soc.* **1985**, *107*, 1141–1146.

(12) McMillin, D. R.; Kirchhoff, J. R.; Goodwin, K. V. *Coord. Chem. Rev.* **1985**, *64*, 83–92.

(13) Edel, A.; Marnot, P. A.; Sauvage, J. P. *Nouv. J. Chim.* **1984**, *8*, 495–498.

(14) Sakaki, S.; Koga, G.; Ohkubo, K. *Inorg. Chem.* **1986**, *25*, 2330–2333.

(15) Dobson, J. F.; Green, B. E.; Healy, P. C.; Kennard, C. H. L.; Pakawatchai, C.; White, A. H. *Aust. J. Chem.* **1984**, *37*, 649–659.

(16) Healy, P. C.; Engelhardt, L. M.; Patrick, V. A.; White, A. H. *J. Chem. Soc., Dalton Trans.* **1985**, 2541–2545.

(17) Sigman, D. S.; Graham, D. R.; D'Aurora, V.; Stern, A. M. *J. Biol. Chem.* **1979**, *254*, 12269–12272.

(18) Sigman, D. S. *Acc. Chem. Res.* **1986**, *19*, 180–186.

(19) Veal, J. M.; Rill, R. L. *Biochemistry* **1988**, *27*, 1822–1827.

(20) Tamilarasan, R.; Ropartz, S.; McMillin, D. R. *Inorg. Chem.* **1988**, *27*, 4082–4084.

(21) Cromer, D. T.; Waber, J. T. *International Tables for X-Ray Crystallography*; Ibers, J. A., Hamilton, W. C., Eds.; Kynoch Press: Birmingham, England, 1974; Vol. IV, pp 71–147.

(22) *CAD 4 Operations Manual*; Enraf-Nonius: Delft, The Netherlands, 1977.

Table III. Bond Distances in Angstroms and Bond Angles in Degrees for $[Cu(bcp)_2]BF_4 \cdot CH_3OH$[a]

Cu–N(100)	2.017 (4)	C(150)–C(192)	1.440 (8)
Cu–N(190)	2.022 (4)	C(160)–C(170)	1.378 (8)
Cu–N(200)	2.032 (4)	C(160)–C(192)	1.420 (8)
Cu–N(290)	2.018 (4)	C(170)–C(180)	1.396 (8)
N(100)–C(101)	1.370 (6)	C(180)–C(181)	1.496 (8)
N(100)–C(110)	1.332 (7)	C(191)–C(192)	1.408 (7)
N(190)–C(180)	1.351 (7)	C(201)–C(202)	1.412 (7)
N(190)–C(191)	1.367 (6)	C(201)–C(291)	1.438 (7)
N(200)–C(201)	1.361 (6)	C(202)–C(230)	1.428 (7)
N(200)–C(210)	1.329 (6)	C(202)–C(240)	1.427 (7)
N(290)–C(280)	1.330 (7)	C(210)–C(211)	1.505 (7)
N(290)–C(291)	1.360 (6)	C(210)–C(220)	1.396 (7)
C(101)–C(102)	1.403 (7)	C(220)–C(230)	1.370 (7)
C(101)–C(191)	1.430 (8)	C(240)–C(250)	1.350 (7)
C(102)–C(130)	1.418 (8)	C(250)–C(292)	1.438 (7)
C(102)–C(140)	1.427 (8)	C(260)–C(270)	1.378 (7)
C(110)–C(111)	1.508 (7)	C(260)–C(292)	1.422 (7)
C(110)–C(120)	1.402 (7)	C(270)–C(280)	1.407 (7)
C(120)–C(130)	1.383 (7)	C(280)–C(281)	1.492 (7)
C(140)–C(150)	1.344 (8)	C(291)–C(292)	1.405 (7)
N(100)–Cu–N(190)	81.8 (2)	N(190)–C(180)–C(170)	121.4 (5)
N(100)–Cu–N(200)	117.9 (2)	N(190)–C(180)–C(181)	117.3 (5)
N(100)–Cu–N(290)	129.8 (2)	C(170)–C(180)–C(181)	121.3 (6)
N(190)–Cu–N(200)	121.0 (2)	N(190)–C(191)–C(101)	116.5 (5)
N(190)–Cu–N(290)	129.3 (2)	N(190)–C(191)–C(192)	123.0 (5)
N(200)–Cu–N(290)	82.0 (2)	C(101)–C(191)–C(192)	120.5 (5)
Cu–N(100)–C(101)	112.7 (4)	C(150)–C(192)–C(160)	124.3 (5)
Cu–N(100)–C(110)	129.9 (3)	C(150)–C(192)–C(191)	117.1 (5)
C(101)–N(100)–C(110)	117.3 (5)	C(160)–C(192)–C(191)	118.5 (5)
Cu–N(190)–C(180)	129.6 (4)	N(200)–C(201)–C(202)	123.4 (5)
Cu–N(190)–C(191)	112.6 (4)	N(200)–C(201)–C(291)	116.8 (4)
C(180)–N(190)–C(191)	117.8 (4)	C(202)–C(201)–C(291)	119.8 (4)
Cu–N(200)–C(201)	112.0 (3)	C(201)–C(202)–C(230)	117.0 (4)
Cu–N(200)–C(210)	129.8 (3)	C(201)–C(202)–C(240)	118.3 (5)
C(201)–N(200)–C(210)	118.2 (4)	C(230)–C(202)–C(240)	124.7 (5)
Cu–N(290)–C(280)	128.7 (3)	N(200)–C(210)–C(211)	116.5 (4)
Cu–N(290)–C(291)	112.7 (3)	N(200)–C(210)–C(220)	121.9 (5)
C(280)–N(290)–C(291)	118.6 (4)	C(211)–C(210)–C(220)	121.6 (5)
N(100)–C(101)–C(102)	123.8 (5)	C(210)–C(220)–C(230)	121.5 (5)
N(100)–C(101)–C(191)	116.2 (5)	C(202)–C(230)–C(220)	117.8 (4)
C(102)–C(101)–C(191)	120.0 (5)	C(202)–C(240)–C(250)	121.7 (4)
C(101)–C(102)–C(130)	117.5 (5)	C(240)–C(250)–C(292)	121.0 (5)
C(101)–C(102)–C(140)	118.4 (5)	C(270)–C(260)–C(292)	117.2 (5)
C(130)–C(102)–C(140)	124.1 (5)	C(260)–C(270)–C(280)	122.1 (5)
N(100)–C(110)–C(111)	117.2 (5)	N(290)–C(280)–C(270)	120.8 (5)
N(100)–C(110)–C(120)	122.6 (5)	N(290)–C(280)–C(281)	118.0 (5)
C(111)–C(110)–C(120)	120.1 (5)	C(270)–C(280)–C(281)	121.2 (5)
C(110)–C(120)–C(130)	120.5 (5)	N(290)–C(291)–C(201)	116.4 (4)
C(102)–C(130)–C(120)	118.1 (5)	N(290)–C(291)–C(292)	123.7 (5)
C(102)–C(140)–C(150)	121.2 (5)	C(201)–C(291)–C(292)	119.9 (4)
C(140)–C(150)–C(192)	121.9 (5)	C(250)–C(292)–C(260)	124.0 (4)
C(170)–C(160)–C(192)	116.7 (5)	C(250)–C(292)–C(291)	118.5 (5)
C(160)–C(170)–C(180)	122.2 (6)	C(260)–C(292)–C(291)	117.5 (4)

[a] Numbers in parentheses are estimated standard deviations in the least significant digits.

condition $I > 3.0\sigma(I)$. Crystal stability was verified. An absorption correction was applied via the empirical method.[23] The minimum transmission factor was 0.46, and the maximum transmission factor was 1.00. Initial atom positions were determined from Patterson maps, and all non-hydrogen atoms were found from subsequent difference Fourier maps. After the positions and anisotropic thermal parameters converged, the positions of the hydrogen atoms were calculated with the assumption of a C–H bond distance of 0.95 Å. In the case of methyl groups, one hydrogen was found from the difference Fourier map, and its positions and the others were adjusted and/or defined by requiring C–C–H bond angles of 109.5° and C–H bond lengths of 0.95 Å. The final values for R and R_w were 0.056 and 0.073, respectively. Positional coordinates for selected atoms are listed in Table II. Pertinent distances and angles are compiled in Table III.

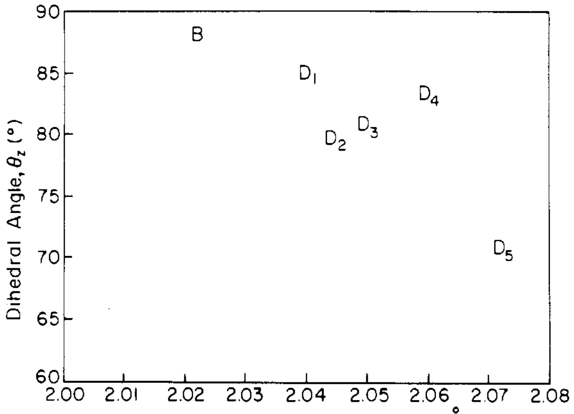

Figure 2. Correlation between the average Cu–N bond distance and the dihedral angle between the ligands. The dihedral angle is taken to be θ_z as defined in ref 15. The compounds represented are (B) $[Cu(bcp)_2]BF_4 \cdot CH_3OH$, ($D_1$) $[Cu(dmp)_2]NO_3 \cdot H_2O$, ($D_2$) $[Cu(dmp)_2]Br \cdot H_2O$, (D_3) $[Cu(dmp)_2]ClO_4$, (D_4) $[Cu(dmp)_2]_2[TCNQ]_2$, and (D_5) $[Cu(dmp)_2]NO_3$. D1–D3 and D5 were plotted from the data in ref 15. Point D4 comes from the data in ref 27.

Results and Discussion

The structure consists of discrete $Cu(bcp)_2^+$ and BF_4^- ions with methanol molecules hydrogen-bonded to the anion. The Cu(I) center is surrounded by an N_4 donor set arranged in a pseudotetrahedral geometry, as can be seen in the ORTEP diagram presented in Figure 1. The average Cu–N distance of 2.022 Å is a crude, but useful, structural indicator. This distance is significantly shorter in the bcp complex than in $Cu(dmp)_2^+$ (2.054 Å),[15,24-27] $Cu(bcp)BH_4$ (2.043 Å),[28] $Cu(dmp)BH_4$ (2.038 Å),[28] $[Cu(phen)_2]ClO_4$ (2.049 Å),[16] or $[Cu(phen)_2]CuBr_2$ (2.053 Å).[16] The dihedral angle between the mean phenanthroline planes is 87.62 (5)°, while the dihedral angles defined by the individual phenyl substituents related to the attached phenanthroline range between 39.33 (23) and 48.26 (16)°. By comparison, the dihedral angle between the mean plane of the phenanthroline moiety and the mean plane of the phenyl substituents is 63.17 (5)° in the structure of the free ligand.[29] In the complex, the phenyl rings are rotated in a disrotatory sense on both ligands, possibly to facilitate stacking interactions.

The principal intermolecular contacts occur as a result of a pseudostacking interaction between molecules related by a glide plane. The upshot is formation of a chain running roughly parallel to the c axis where the interplanar angle between the stacked phenanthroline is 153.03 (13)°. However, the closest contacts involve the phenyl substituents. Atom–atom distances of interest in this regard include the following: C(170)–C(232), 3.25 Å; C(131)–C(262), 3.38 Å; C(132)–C(262), 3.43 Å; C(166)–C(220), 3.45 Å.

The presence of the phenyl substituents probably prevents more extensive stacking such that the phenanthroline cores eclipse each other, as is observed in the structure of $[Cu(phen)_2]ClO_4$.[16] In a previous report we suggested that such stacking facilitates a flattening distortion whereby the dihedral angle between mean ligand planes is reduced.[30] In line with this reasoning, the dihedral angle of the bcp complex is 87.62 (5)°, hardly different from the 90° angle of an idealized, pseudotetrahedral complex. Another effect, which could be important in determining the driving force for the flattening distortion, is that the Coulombic forces within the lattice may be reduced due to the relatively large effective radius of the $Cu(bcp)_2^+$ cation.

---

(23) Walker, N.; Stuart, D. *Acta Crystallogr., Sect. A* **1983**, *A39*, 158–166.

(24) Hämäläinen, R.; Turpeinen, U.; Ahlgrén, M.; Raikas, T. *Finn. Chem. Lett.* **1978**, 199–202.

(25) Hämäläinen, R.; Ahlgrén, M.; Turpeinen, U.; Raikas, T. *Cryst. Struct. Commun.* **1979**, *8*, 75–80.

(26) Dessy, G.; Fares, V. *Cryst. Struct. Commun.* **1979**, *8*, 507–510.

(27) Hoffmann, S. K.; Corvan, P. J.; Singh, P.; Sethulekshmi, C. N.; Metzger, R. M.; Hatfield, W. E. *J. Am. Chem. Soc.* **1983**, *105*, 4608–4617.

(28) Green, B. E.; Kennard, C. H. L.; Smith, G.; Elcombe, M. M.; Moore, F. H.; James, B. D.; White, A. H. *Inorg. Chim. Acta* **1984**, *83*, 177–189.

(29) Klemens, F. K. M.S. Dissertation, Purdue University, West Lafayette, IN, 1989.

(30) Goodwin, K. V.; McMillin, D. R.; Robinson, W. R. *Inorg. Chem.* **1986**, *25*, 2033–2036.

If the average observed Cu–N bond distance is plotted against the dihedral angle between ligands, an interesting trend emerges for the Cu(dmp)$_2^+$ and Cu(bcp)$_2^+$ systems (Figure 2). The Cu–N distance increases with the degree of flattening. This is reasonable because interligand repulsions between opposing methyl groups are expected to increase as the dihedral angle decreases. Consistent with this interpretation, the Cu(phen)$_2^+$ system subtends a wide range of dihedral angles with little change in the average Cu–N bond distance.[16] The trend in the data reported in Figure 2 also strongly supports the contention that lattice forces, rather than intramolecular bonding interactions, are responsible for the flattening distortion.[30]

The fact that the dihedral angles subtended by the phenyl groups are much less than 90° is in accord with a previous analysis of the charge-transfer absorption intensity.[4] Although the interplanar angles are smaller in the complex than in the free ligand, it is not clear whether this occurs as a result of an intramolecular π-bonding interaction or a lattice effect. In any event, neither the intramolecular nor the intermolecular forces that exist in the solid state suffice to overcome the severe hydrogen atom/hydrogen atom contacts required for the phenyl substitutents to be coplanar with the phenanthroline core. It remains to be seen whether intercalation into DNA depends upon an in-plane orientation of the phenyl groups.

Acknowledgment. This research was supported by the National Science Foundation through Grant No. CHE-8719538 and by the National Institutes of Health through Grant No. GM 22764.

Supplementary Material Available: Tables listing positional parameters and their estimated standard deviations, bond angles and bond distances, general temperature factor expressions, and least-squares planes along with their dihedral angles (12 pages); a table of calculated and observed structure factors (26 pages). Ordering information is given on any current masthead page.

Contribution from the Section of Chemistry,
Karl Marx University, DDR-7010 Leipzig, GDR,
Departments of Chemistry and Physics and
Liquid Crystal Institute, Kent State University,
Kent, Ohio 44242, and Department of Chemistry,
University of Virginia, Charlottesville, Virginia 22901

Powder EPR of Tris(diethylthioselenocarbamato)- and Tris(diethyldiselenocarbamato)iron(III) Diluted in the Analogous Cobalt(III) and Indium(III) Complex Matrices

Wolfgang Dietzsch,[1a] Norman V. Duffy,*,[1b]
Edward Gelerinter,*,[1c] and Ekk Sinn*,[1d]

Received September 15, 1988

The tris(diorganodichalcogenocarbamato)iron(III) complexes are a well-characterized ${}^6A_1 \rightleftharpoons {}^2T_2$ spin-crossover system and the relative population of high-spin and low-spin electronic configurations depends on the coordinating chalcogen (O, S, or Se), temperature, pressure, physical state (solution or solid, solvated or without solvents of crystallization), and the nature of the organic substituents.[2]

While Mössbauer spectroscopy sees only the averaged spectra of the two electronic configurations,[3] the EPR[4,5] and infrared spectroscopic[4,6] time scales are sufficiently short to see separate signals from both high-spin (${}^6A_1$) and low-spin (${}^2T_2$) states. The potential problem of intermolecular spin-coupling between adjacent Fe(III) (3d^5) atoms in the EPR has been addressed by diluting the sample in a host matrix of the corresponding Co(III) (3d^6) complex or a frozen glass.[4,7,8]

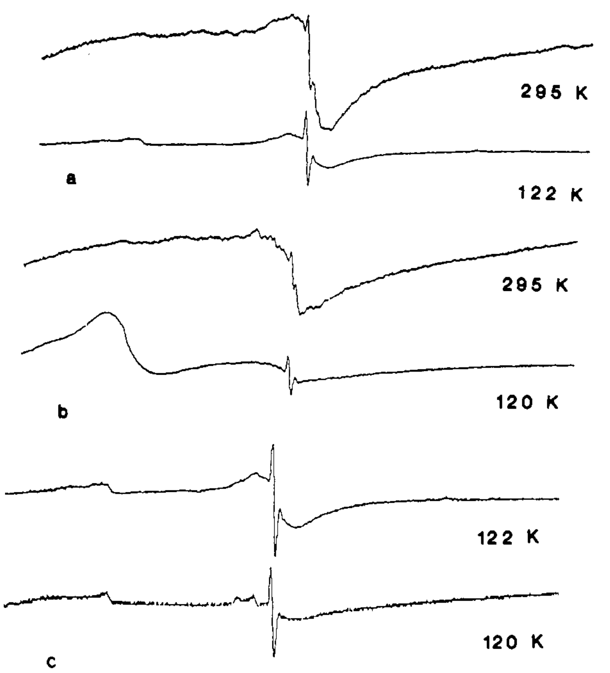

Figure 1. Powder EPR (X-band) spectra of (a) 1% Fe(SSeCN(C$_2$H$_5$)$_2$)$_3$ in a solid matrix of Co(SSeCN(C$_2$H$_5$)$_2$)$_3$ as a function of temperature, (b) 1% Fe(SSeCN(C$_2$H$_5$)$_2$)$_3$ in a solid matrix of In(SSeCN(C$_2$H$_5$)$_2$)$_3$ as a function of temperature, and (c) 1% Fe(SSeCN(C$_2$H$_5$)$_2$)$_3$ in a solid matrix of Co(SSeCN(C$_2$H$_5$)$_2$)$_3$ (upper spectrum) and 1% Fe(Se$_2$CN(C$_2$H$_5$)$_2$)$_3$ in Co(Se$_2$CN(C$_2$H$_5$)$_2$)$_3$ (lower spectrum) at the temperature indicated. Sweep width is from 510 to 6310 G. Amplitudes have been normalized so that the narrow line at $g = 2$ has approximately the same amplitude in all spectra.

We report the first EPR spectra of magnetically dilute tris(thioselenocarbamato)- and tris(diselenocarbamato)iron(III) complexes.

Experimental Section

Each of the following complexes have been prepared by methods similar to those reported in the literature and gave satisfactory elemental analyses: Fe(SSeCN(C$_2$H$_5$)$_2$)$_3$;[9,10] Co(SSeCN(C$_2$H$_5$)$_2$)$_3$ and In(SSeCN(C$_2$H$_5$)$_2$)$_3$;[9] Fe(Se$_2$CN(C$_2$H$_5$)$_2$)$_3$;[11,12] Co(Se$_2$CN(C$_2$H$_5$)$_2$)$_3$;[13-15] In(Se$_2$CN(C$_2$H$_5$)$_2$)$_3$.[16]

Magnetic Data. Magnetic susceptibilities (4–320 K) were measured on a SQUID magnetometer. The calibration and method of operation are described elsewhere.[17]

EPR Spectra. The samples were sealed in 4-mm-o.d. quartz tubes under approximately 0.5 atm of nitrogen. Data were obtained by using an IBM 200D-SRC spectrometer with an ER 044 MRDH X-band microwave bridge. The temperature was controlled with an IBM ER 4111

---

(1) (a) Karl Marx University. (b) Department of Chemistry, Kent State University. (c) Department of Physics and Liquid Crystal Institute, Kent State University. (d) University of Virginia.

(2) Coucouvanis, D. *Prog. Inorg. Chem.* **1970**, *11*, 233; **1979**, *26*, 301.

(3) Merrithew, P. B.; Rasmussen, P. G. *Inorg. Chem.* **1972**, *11*, 325.

(4) Hall, G. R.; Hendrickson, D. N. *Inorg. Chem.* **1976**, *15*, 607.

(5) Flick, C.; Gelerinter, E. *Chem. Phys. Lett.* **1973**, *23*, 422. Flick, C.; Gelerinter, E.; Zimmerman, J. B.; Duffy, N. V. *Inorg. Chem.* **1976**, *15*, 2945.

(6) Butcher, R. J.; Ferraro, J. R.; Sinn, E. *J. Chem. Soc., Chem. Comm.* **1976**, 910; *Inorg. Chem.* **1976**, *15*, 2077.

(7) Rickards, R.; Johnson, C. E.; Hill, H. A. O. *J. Chem. Phys.* **1970**, *53*, 3118.

(8) Perry, D. L.; Wilson, L. J.; Kunze, K. R.; Maleki, L.; Deplano, P.; Trogu, E. F. *J. Chem. Soc., Dalton Trans.* **1981**, 1294.

(9) Heber, R.; Kirmse, R.; Hoyer, E. *Z. Anorg. Allg. Chem.* **1972**, *393*, 159.

(10) Dietzsch, W.; Boyd, D. L.; Uhrich, D. L.; Duffy, N. V. *Inorg. Chim. Acta* **1986**, *121*, 19.

(11) Cervone, E.; Camessei, F. D.; Luciani, M. L.; Furlani, C. *J. Inorg. Nucl. Chem.* **1969**, *31*, 1101.

(12) DeFilippo, D.; Depalano, P.; Diaz, A.; Steffe, S.; Trogu, E. F. *J. Chem. Soc., Dalton Trans.* **1977**, 1566.

(13) Bond, A. M.; Colton, R.; Mann, D. R.; Moir, J. E. *Aust. J. Chem.* **1986**, *39*, 1385.

(14) Furlani, C.; Cervone, E.; Camassei, F. D. *Inorg. Chem.* **1968**, *7*, 265.

(15) Pan, W. H.; Fackler J. P., Jr.; Chen, H. W. *Inorg. Chem.* **1981**, *20*, 856.

(16) Jensen, K. A.; Krishnan, V. *Acta Chem. Scand.* **1968**, *21*, 2904.

(17) O'Connor, C. J.; Sinn, E.; Cukauskas, E.; Deaver, B. S., Jr. *Inorg. Chim. Acta* **1979**, *32*, 29. O'Connor, C. J.; Deaver, B. S., Jr.; Sinn, E. *J. Chem. Phys.* **1979**, *70*, 5161.

0020-1669/89/1328-3079$01.50/0